This article was downloaded by:
On: *22 January 2011*
Access details: *Access Details: Free Access*
Publisher *Taylor & Francis*
Informa Ltd Registered in England and Wales Registered Number: 1072954 Registered office: Mortimer House, 37-41 Mortimer Street, London W1T 3JH, UK

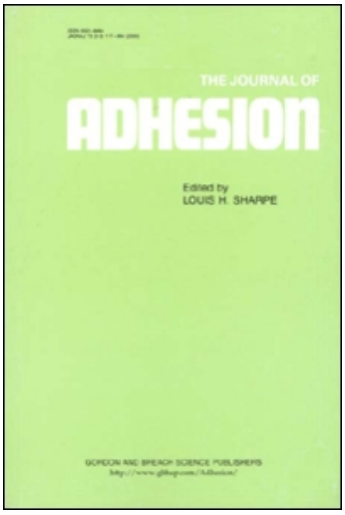

The Journal of Adhesion

Publication details, including instructions for authors and subscription information:
http://www.informaworld.com/smpp/title~content=t713453635

The Body's Response to Inadvertent Implants: Respirable Particles in Lung Tissues

R. Baier[a]; A. Meyer[a]; D. Glaves-rapp[b]; E. Axelson[a]; R. Forsberg[a]; M. Kozak[a]; P. Nickerson[a]
[a] Industry/University Center for Biosurfaces, State University of New York at Buffalo, Buffalo, NY, USA [b] Roswell Park Cancer Institute, Buffalo, NY, USA

To cite this Article Baier, R. , Meyer, A. , Glaves-rapp, D. , Axelson, E. , Forsberg, R. , Kozak, M. and Nickerson, P.(2000) 'The Body's Response to Inadvertent Implants: Respirable Particles in Lung Tissues', The Journal of Adhesion, 74: 1, 103 — 124
To link to this Article: DOI: 10.1080/00218460008034526
URL: http://dx.doi.org/10.1080/00218460008034526

PLEASE SCROLL DOWN FOR ARTICLE

Full terms and conditions of use: http://www.informaworld.com/terms-and-conditions-of-access.pdf

This article may be used for research, teaching and private study purposes. Any substantial or systematic reproduction, re-distribution, re-selling, loan or sub-licensing, systematic supply or distribution in any form to anyone is expressly forbidden.

The publisher does not give any warranty express or implied or make any representation that the contents will be complete or accurate or up to date. The accuracy of any instructions, formulae and drug doses should be independently verified with primary sources. The publisher shall not be liable for any loss, actions, claims, proceedings, demand or costs or damages whatsoever or howsoever caused arising directly or indirectly in connection with or arising out of the use of this material.

J. Adhesion, 2000, Vol. 74, pp. 103–124
Reprints available directly from the publisher
Photocopying permitted by license only

© 2000 OPA (Overseas Publishers Association) N.V.
Published by license under
the Gordon and Breach Science
Publishers imprint.
Printed in Malaysia.

Downloaded At: 09:58 22 January 2011

The Body's Response to Inadvertent Implants: Respirable Particles in Lung Tissues

R. BAIER[a,*], A. MEYER[a], D. GLAVES-RAPP[b], E. AXELSON[a], R. FORSBERG[a], M. KOZAK[a] and P. NICKERSON[a]

[a]*Industry/University Center for Biosurfaces, State University of New York at Buffalo, Buffalo, NY 14214-3007, USA;*
[b]*Roswell Park Cancer Institute, Buffalo, NY, USA*

(Received 21 February 2000; In final form 16 August 2000)

Instillation of respirable glass fibers to rat lungs served as an *in vivo* model for the detection and evaluation of differential local biological responses to particulate matter in the deep lung. Three compositions of vitreous glass, stonewool, and refractory fiber materials (MMVF 10, HT, and RCF1a) were harvested with surrounding lung tissues and examined both histologically and by physical/chemical assays to correlate the observed differential dissolution events with specific biological responses associated with each material. Specimens at 2-days, 7-days, 30-days and 90-days post-instillation were compared from at least three rats for each condition and for phosphate-buffered-saline controls. HT fiber surface and bulk chemistry uniquely allowed direct histochemical visualization of fiber degradation steps by Prussian Blue staining, while multiple attenuated internal reflection infrared spectroscopy and energy-dispersive X-ray analysis of unfixed, fresh lung lobe slice surfaces revealed the concurrent biochemical changes. Insulation glass (MMVF 10) dissolved most quickly in extracellular compartments, as well as after phagocytosis of small fragments; stonewool (HT) was externally thinned by surrounding phagocytes and fragmented into shorter lengths engulfable by macrophages; refractory ceramic (RCF1a) resisted both external dissolution and macrophage uptake, becoming embedded in granulomatous nodules. It is clear from these results that the lung can process inadvertently respired particulates in different ways dependent on the specific compositions of the particles.

The animal model and analytical scheme reported here also show substantial promise for evaluating the effects of bioaerosols, and synergistic effects of respirable toxins with particulates, and consequences of dental aspirates into the lung.

Keywords: Particles; Lungs; Glass; Dissolution; Stains; Fibers

*Corresponding author. Tel.: 716-829-3560, Fax: 716-835-4872, e-mail: baier@acsu.buffalo.edu

INTRODUCTION

Respirable particulate matter, and especially asbestos, has a long history of significant health risk, including the causation of cancer [1]. If history is not to be repeated, the bioevaluation of alternative materials that may become environmental particles when used in construction and fabrication becomes of paramount importance. This study used physical–chemical and histochemical methods to determine the location, physiologic environment, tissue reaction to, and durability of 3 types of respirable fiberglass as a model for the pattern by which other particles, inadvertently delivered to the lungs or other body tissues, might be biologically processed. Particles that persist undissolved and resistant to cellular engulfment (phagocytic action by macrophages) have the potential to cause chronic health hazards [1–6]. The three types of fiberglass were selected based on prior observations of their significantly different dissolution rates *in vitro* in model lung fluid [1, 7].

Prior research has focused mainly upon *in vitro* correlates with physical persistence of fibers in the lung [1, 3, 8, 9], not upon characterization of the *in vivo* physiologic milieu and cellular components which determine whether fibers are dissolved or if they remain and present a potential biohazard [10–13]. Furthermore, live animals proved to be necessary for studies of the fate of glass fibers, after other reports showed that the behavior of particles *in vitro* does not necessarily predict their behavior in the animal [8–13].

The study reported here utilized intratracheal delivery of particles to rat lungs, tissue preservation, and evaluation of particles in tissues, two to ninety days after instillation. Other organs also were retrieved to determine whether phagocytes transported particles away from the lungs over time.

The results clearly showed composition-dependent differences in the paths of biological processing of these fibers, with the specific involvement of phagocytic cells that could externally digest and fragment a material (HT stonewool) otherwise insoluble in extracellular fluid.

Work currently in progress includes retrieval of lung macrophages and particles by lung lavage, 2 to 90 days after instillation. The interactions of living macrophages and glass fibers are being studied

Downloaded At: 09:58 22 January 2011

by localized pH indicators [14, 15], confocal microscopy, and immunohistopathology.

METHODS AND MATERIALS

Animal Model

Fisher 344/Charles River Rats (female) were selected, since this species/strain is the standard model in published studies on interaction of particles with the lung. Rats are of sufficient size to permit visual and tactile monitoring of intratracheal tube insertion into the oropharynx without magnification. Three main types of particles with different rates of dissolution *in vitro*, with known and suspected differential impacts on lung physiology [7] were instilled. Groups of at least 3 rats per particle type accommodated variation between individuals and provided scientifically analyzable and valid data. For each of the three particle types, there were groups of 3 test rats per each of 4 post-instillation times (2, 7, 30 and 90 days), for a total of 36 animals. A single series of control rats instilled with carrier fluid (phosphate–buffered saline) was used per each of the 4 sample times [12 rats]. One additional group of untreated rats served as a control group [3 rats]. Additional time points immediately after instillation were tested to develop the various animal tissue harvest, preservation, and analysis protocols [24 rats].

Downloaded At: 09:58 22 January 2011

Vitreous Fibers

Three types of vitreous fibers were used: refractory ceramic fiber [RCF1a], insulation fiber [MMVF 10], and stonewool fiber [HT]. Fibers already sorted for their respirable size (averaging 1 micron diameter, 20 microns in length) were obtained from fiberglass manufacturers. Fiber sizes and general compositions were confirmed by scanning electron microscopy (SEM) and energy-dispersive X-ray (EDXray) analysis. Published dissolution constants for the three types of fiberglass are given in Table I.

For each group of 3 rats, a mass of fibers sufficient for instillation of the group was measured into a 4 ml vial and delivered to the animal

TABLE I Dissolution rates of fiberglasses used in rat lung instillation experiments

Fiberglass type	*Dissolution constant* [$ng/cm^2/h$]	*Literature reference*
MMVF 10	300	[1]
HT	59	[7]
RCF1a	3	[1]

surgery facility. Just prior to instillation, saline was added to the vial and the particle suspension was vortexed briefly to distribute the fibers evenly. The initial HT fiber dispersion was unstable but this was overcome by prior mild glow-discharge treatment [16], which did not compromise the relevance of the data to actual environmental exposures.

A dose of 1.2 mg of particles in 0.2 ml saline was instilled in each rat. Each instillation control rat received 0.2 ml saline intratracheally. Other control rats received no treatment.

Downloaded At: 09:58 22 January 2011

Particle-instillation Procedure

A blunt-end, 18-gauge intubation needle was gently inserted into the trachea of the anesthetized rat. After insertion, the particle suspension was instilled into the trachea. Instillation ensured that a prescribed dose of particles was accurately delivered to the target organ in sufficient particle numbers with potential to cause discernable tissue reactions.

After designated post-instillation time periods (2–90 days), each animal was again anesthetized prior to perfusion, and then euthanized with an overdose of the original anesthetic prior to tissue harvesting. Blood samples were obtained to ascertain the relative populations of leukocytes (white blood cells): polymorphonucleocytes, lymphocytes, monocytes, eosinophils, and basophils. This type of analysis is called a "differential blood analysis" [17], whereby the percentages of the different types of leukocytes are determined. Significant shifts in blood cell populations can be signals of inflammatory or immune reactions, or reveal problems of infection or toxin contamination that would compromise the interpretations of the subsequent analyses.

After blood samples were obtained, saline was perfused into the rat's left ventricle to displace blood from the vascular system, most importantly from microvessels in the lungs and from other organs. After saline perfusion, one lung lobe was isolated, ligated, and excised for subsequent infrared spectroscopy and SEM/EDXray analysis. The remaining lung lobes then were perfused and chemically crosslinked ("fixed") with formalin. The lungs were inflated with formalin *via* the trachea prior to final dissection and immersion in formalin-filled containers. Thoracic lymph nodes and abdominal organs (spleen, kidney, liver) also were excised and fixed in formalin for later evaluation of fiber transport from the lungs.

The animals in this study were used in accordance with regulations and standards promulgated by the New York State Department of Health, the United States Department of Agriculture, the Public Health Service, Roswell Park Cancer Institute, and the University at Buffalo. Pain or discomfort to animals was limited to that which was unavoidable in the conduct of scientifically valid research. To the best of our knowledge, the studies did not unnecessarily duplicate any other in the published literature. The animal species, numbers and procedures used were the most appropriate for the investigation performed.

Downloaded At: 09:58 22 January 2011

Analysis of Fibers and Surrounding Tissues

Lungs from rats with intratracheally-instilled glass fibers were harvested at 2, 7, 30 and 90 days post-instillation. Lung lobes from each animal were histologically processed and stained with hematoxylin and eosin (H&E), Masson Trichrome, and Prussian Blue reagents. The Prussian Blue stain yielded superb visualization of the HT fibers at various stages of their deterioration within the lung.

Fresh freeze-fractured lung lobes and fragments were examined by SEM and EDXray analysis, as-prepared and after glow-discharge-plasma processing for "relief" exposure of the inorganic fibers from their embedding organic tissues. Fresh lung lobe slices (saline-perfusion only prior to lung lobe excision; no paraffin embedment) were applied to the faces of germanium internal reflection crystals and dried under ambient laboratory conditions. The chemistries of lung tissue slices on the germanium plates were determined using

multiple-attenuated-internal-reflection-infrared (MAIR-IR) spectroscopy. The IR spectra were analyzed for absorptions related to protein (1650 and 1540 cm^{-1}), lipid (1750–1700 cm^{-1}), and carbohydrate and silica moieties (1020–1080 cm^{-1}). Collagen protein was differentiated from glycoproteinaceous extracellular substances by the IR absorption band at 1240 cm^{-1}, attributed to the uniquely high hydroxyproline content of the collagen. Following MAIR-IR spectroscopy, the tissue slices were rehydrated and removed from the germanium plates. A "print" (residue) of the lung tissue remaining adhesively bonded on the plate was examined again by MAIR-IR and then by SEM and EDXray techniques.

RESULTS

Downloaded At: 09:58 22 January 2011

All three types of vitreous fiber inclusions could be identified in H&E and Masson Trichrome-stained sections, 2 and 7 days post-instillation in deep lung tissue. They were mainly located within granulomas, collections of tightly-packed phagocytic cells surrounding the individual fibers. Figure 1a is a scanning electron microscopic [SEM] view of an unstained, freeze-fractured lung lobe, in a region where a refractory ceramic fiber is exposed near the surface. Figure 1b is a series of elemental maps for the major components of the fiber and surrounding tissue seen in the SEM view. It is noteworthy that calcium was *not* detectable in the RCF1a fiber. It was extremely difficult to resolve the RCF1a and MMVF 10 fibers in histological sections, even with the aid of stains, but the HT fiber type did yield positive results from direct fiber-staining attempts. Despite even greater problems of resolving micrometer-level details with infrared illumination, the application of Fourier Transform Infrared Microscopy [18] also has been useful in identifying the different chemistries of the embedded fibers, their surrounding granulomatous nodules, and the general lung tissue structures. Preliminary results from IR microscopic characterization of glass fibers in lung sections are addressed in the Discussion.

Surveys of stained sections, prepared from the complete range of lung samples and viewed by light microscopy, indicated that granulomatous nodules generally diminished in number, size, and staining intensity with increasing post-instillation time for the

insulation fibers (MMVF 10) and stonewool (HT). Nodules persisted and may have even increased with time in the 30–90 day post-instillation cases for the refractory ceramic fibers (RCF1a). Quantitative image analysis is in progress, to examine the prospects that insoluble refractory fibers become protected from further cellular attack in the interstitial spaces by their connective tissue and scar capsules. In the cases examined here, by the 90-day observation time, most of the granulomas around the MMVF 10 and HT fibers were resolved and only few persistent fibers of these types were found embedded and integrated in flat tissue capsules. At the light microscopic level, the HT fragments also had lost most of their Prussian Blue staining intensity, by 90-days post-instillation.

Results of Microscopic Analyses

Results of light microscopy, SEM, and EDXray analyses are reported in this section.

Downloaded At: 09:58 22 January 2011

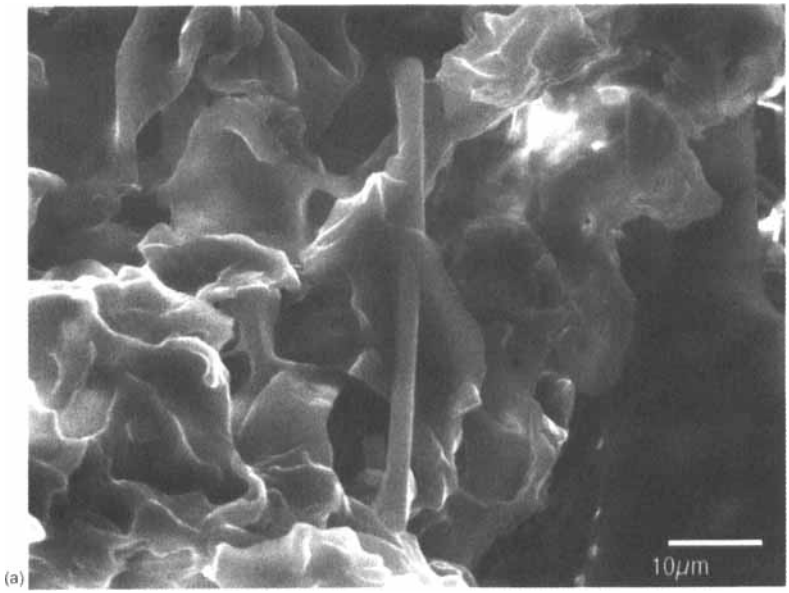

FIGURE 1 (a) Scanning electron micrograph for RCF1a fiber in rat lung for 30 days. (b) Elemental maps acquired by energy-dispersive X-ray analysis for constituents of fiber and lung tissue structures shown in SEM micrograph.

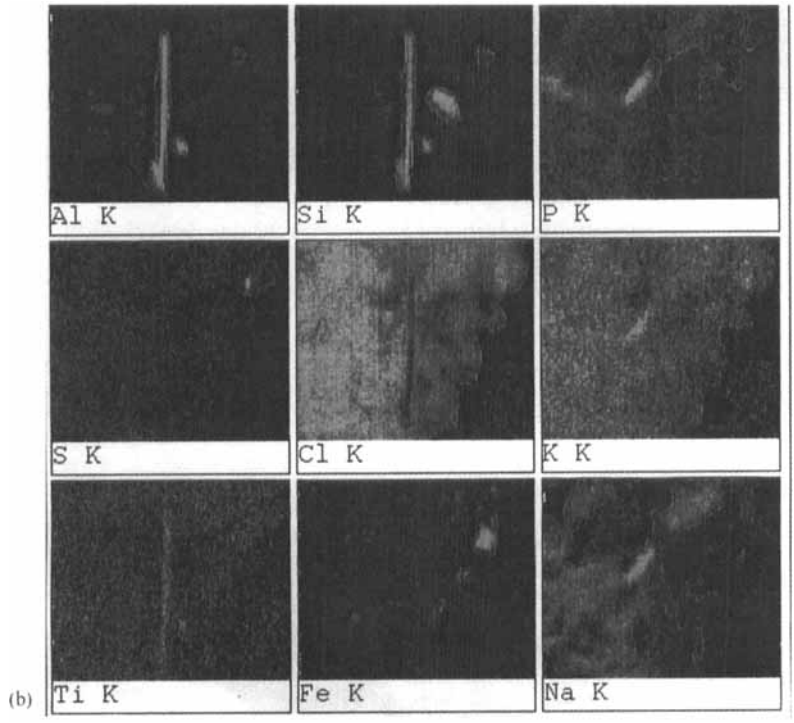

FIGURE 1 (Continued). (See Color Plate I).

Downloaded At: 09:58 22 January 2011

The HT fibers uniquely gave a bright blue-purple reactive coloration when the tissue preparation was stained with Prussian Blue dye. This allowed rapid location of the small fibers and direct visualization of fiber breakdown. Light microscopic views, such as that shown in Figure 2, demonstrated that HT fiber breakdown often occurred in two steps: (1) localized fiber breakage or digestion at locations where closely approximated phagocytes were associated with selectively thinning fiber sites; and (2) generalized dissolution over time in a patchy fashion along the fiber. Broken segment lengths usually appeared in close proximity to the adjacent, surrounding reactive cells.

Figure 3 shows such fibers transferred from a fresh lung lobe slice to a smooth germanium internal reflection prism, in a "lung print" left behind when this tissue was gently peeled from the prism after multiple attenuated internal reflection infrared analysis. In Figure 3, the fibers

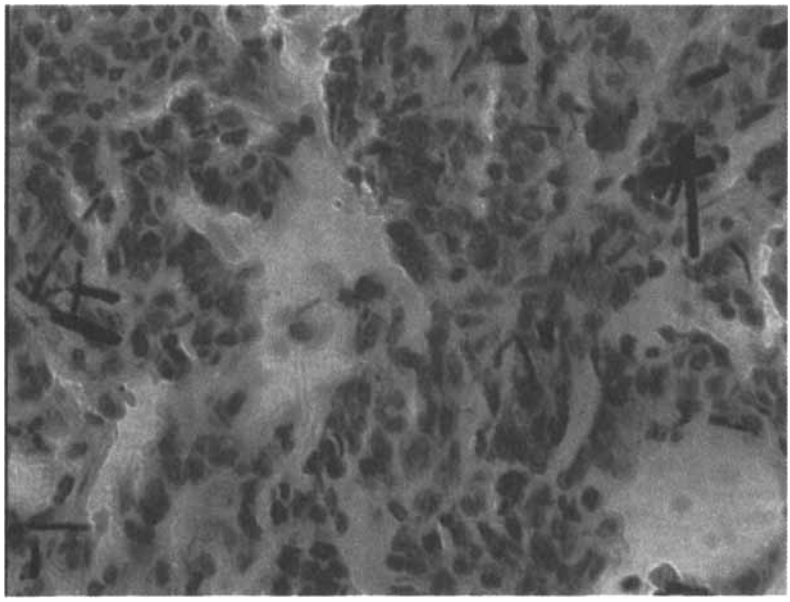

FIGURE 2 Light microscopic view of HT fibers in rat lung 2 days after instillation. Note irregular edges and ends of broken fiber segments in upper-left quadrant of this view. Average diameter of fibers seen here is 1 micrometer.

Downloaded At: 09:58 22 January 2011

seen are from freshly-harvested lung tissue 7-days post-instillation with HT (stonewool). It is noteworthy that these fiber surfaces appeared, at only 7 days, already significantly micro-pitted and porous. In contrast, the exteriors of RCF1a refractory fibers, similarly examined even at the longer 30- and 90-day observation points, remained superficially smooth and optically dense.

Figure 4a is a scanning electron microscopic view of a freeze-fractured, glow-discharge-relieved deep lung tissue segment 7-days post-instillation of HT fiber. Such exposed HT fiber surfaces usually were seen to be pitted and porous. Figure 4b confirms the chemistry of HT fibers as published and compared with numerous other vitreous fiber types [7] by EDXray analysis. HT is uniquely rich in calcium as well as having the high amounts of aluminum and silicon characterizing refractory RCFla fibers [7].

Figure 5 is the elemental map for this same tissue region, where the co-locations of aluminum, silicon, and calcium within the HT fiber

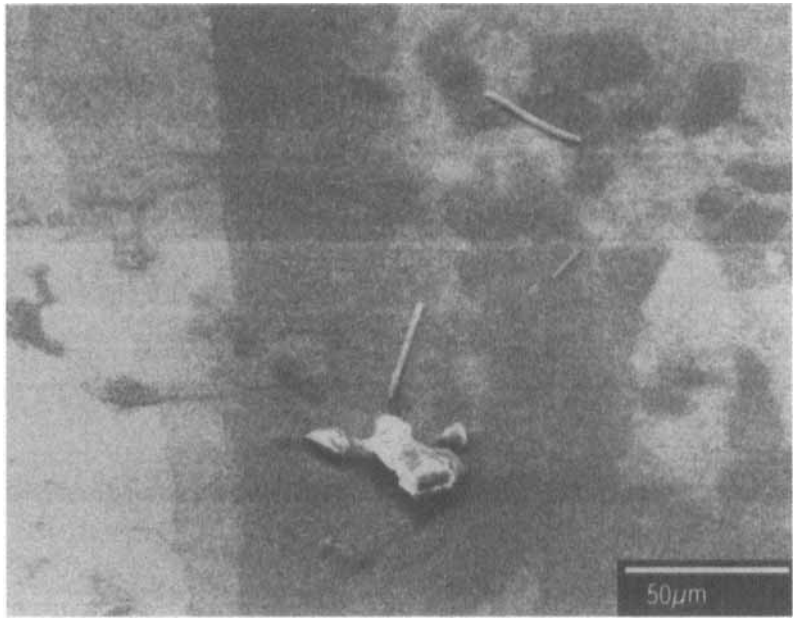

FIGURE 3 Scanning electron micrograph of HT fibers transferred from fresh lung slice to germanium internal reflection prism. Tissue slice was peeled from the prism after analysis by MAIR-IR spectroscopy. The IR spectrum of the residue seen here also was obtained.

Downloaded At: 09:58 22 January 2011

body are obvious. However, the aluminum and silicon elemental signals are considerably less intense than obtained under the same conditions for similarly-sized RCF1a fibers (compare this 7-day result for HT with the 30-day result for RCF1a, Fig. 1b). These energy-dispersive X-ray results also independently confirmed the light-microscopic findings, where Prussian Blue staining showed rapid and substantial loss of apparent HT fiber mass in regions of high phagocytic cellular abundance.

Many of the 7-day specimen SEM views of HT fibers showed narrowing fiber diameters (necking) adjacent to the regions of closest cell membrane approximation, suggesting an active digestive process that did not require fiber internalization or engulfment [19].

Some scanning electron microscopic views of 30-day HT-instilled-lung specimens showed still-smooth fibers "torn" from adjacent tissue

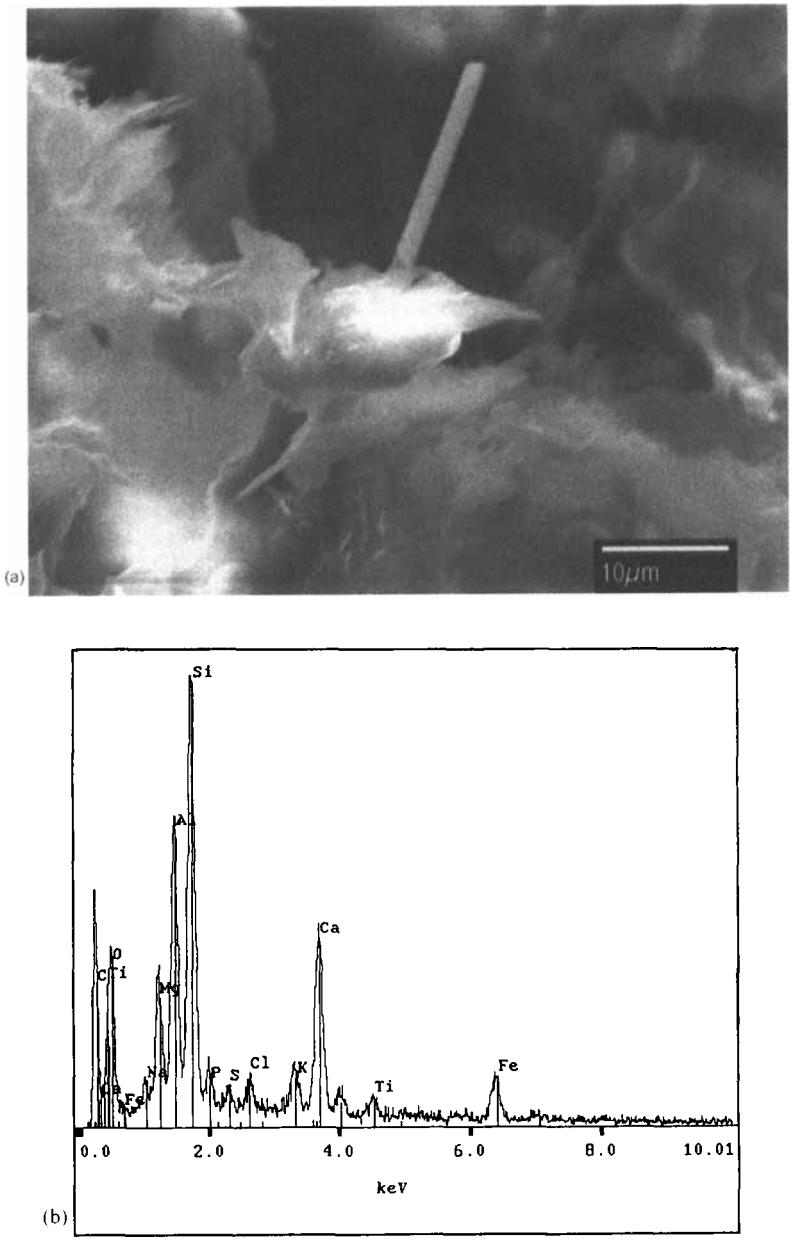

FIGURE 4 (a) Scanning electron micrograph for HT fiber in rat lung for 7 days. (b) Energy-dispersive X-ray spectrum of fiber and lung tissue shown in SEM micrograph.

Downloaded At: 09:58 22 January 2011

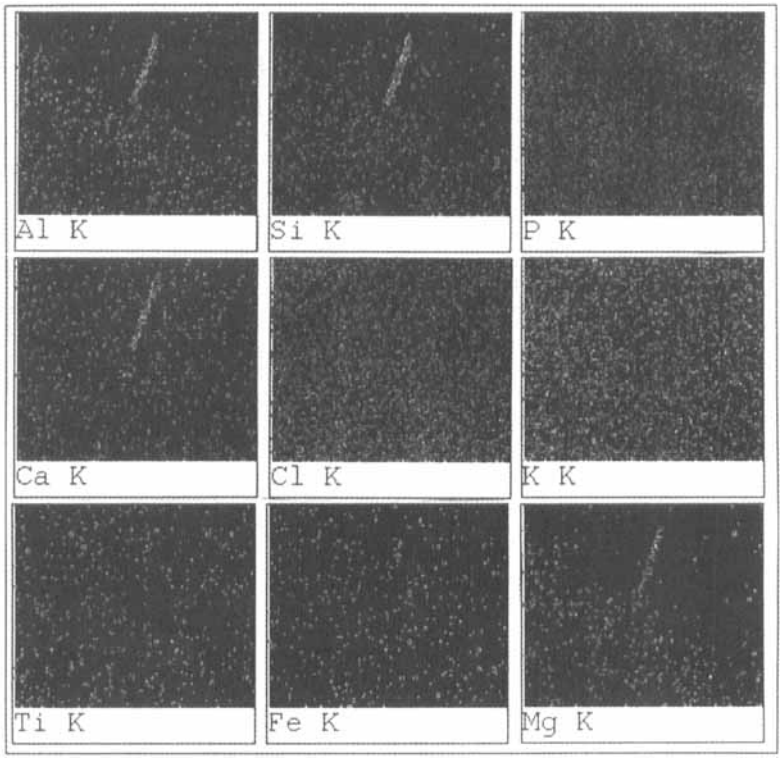

FIGURE 5 Elemental maps acquired by energy-dispersive X-ray analysis for constituents of fiber and lung tissue structures shown in Figure 4a. Compare with data obtained for refractory ceramic fiber RCF1a in tissue for 30 days (Fig. 1b). (See Color Plate II).

crypts. Such SEM views correlated with "scar" sites seen in the stained tissue sections where fiber-shaped voids were present as well as irregularly-shaped, still-present fiber fragments nearby. The longer-preserved HT fibers apparently had been protected from the scavenging phagocytes by collagen and fibroblasts of the usually dominant "foreign body response" of living tissues [20, 21]. Collagen was identified in these capsules by its characteristic blue–green color after Masson Trichrome staining of tissue sections. This result shows that general body fluids, extracellular matrix, or tissue chemistry away from reactive phagocytes, were not responsible for the degradation of HT fibers seen in the rat lungs examined in the current study.

Downloaded At: 09:58 22 January 2011

Results of Infrared Spectroscopy

As illustrated in Figure 6, the removal of the lung slices from the faces of the analytical IR prisms correlated with a spectral loss of absorption bands typical of the collagen-based lung tissue scaffolding, leaving behind abundant glycoproteinaceous extracellular substances and variable amounts of lung surfactant (lipid).

Labels on Figure 6 designate the covalent chemical absorption bands characterizing the faces of fresh lung slices placed on germanium prisms, examined by multiple attenuated internal reflection infrared [MAIR-IR] spectroscopy. The spectra of as-placed segments (Fig. 6a) and the same specimens after peeling the bulk

Downloaded At: 09:58 22 January 2011

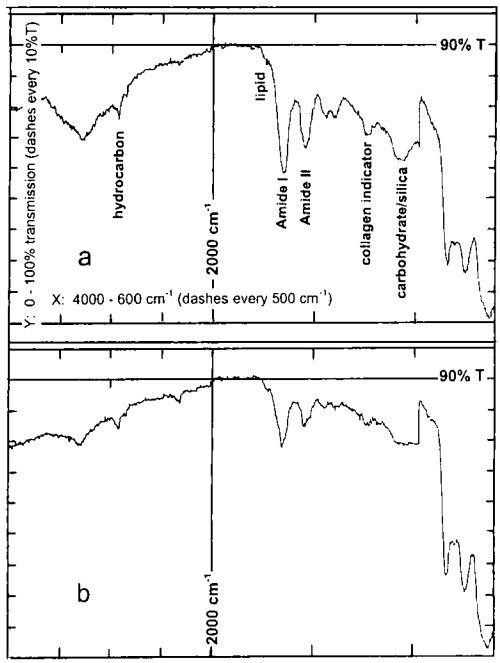

FIGURE 6 (a) Infrared spectrum, obtained by multiple-attenuated internal reflection technique, of rat lung tissue (HT, 2 days) on germanium internal reflection prism. (b) IR spectrum of residue on germanium prism after rehydrating and removing slices of lung tissue. Note that 100% of the lung surfactant (lipid component indicated by absorption between 1700 and 1750 cm^{-1}) remains as residue after the tissue is removed. Bands associated with protein and carbohydrate lost an average 61% of their intensities. Figure 2 is a SEM micrograph of the residue on the prism.

tissues from the prisms to leave behind "lung prints" always produced records of the sort noted in Figure 6b. These IR spectra reveal how removal of the bulk tissue selectively diminished the collagen-related absorption at about 1240 cm^{-1}, while leaving behind most of the lung surfactant phase with its lipid-related absorption at about 1730 cm^{-1}. Specific absorption bands for harvested lung lobe slices were compared with one another and from lung-to-lung and fiber-type-to-fiber-type throughout the 2-day to 90-day experimental period.

Figure 7 charts the most revealing of these comparisons, the ratio of protein to extracellular matrix materials (polysaccharide-rich) over time. The significantly greater and persisting abundance of protein in the refractory fiber RCFla-instilled lungs correlated with the formation and persistence of granulomas surrounding these dissolution-resistant fibers, as viewed by light microscopy of stained sections from the same lungs. It is helpful, here, to reinspect Figure 1a (a SEM view) and Figure 1b (a corresponding energy-dispersive X-ray elemental map) for fiber segments in a freeze-fractured and then glow-discharge-relieved lung specimen from a rat harboring RCF1a fibers for 30 days. Intense signals for aluminum, silicon and titanium characterize the fiber; weaker signals for phosphorus, sodium and iron characterize the cells of the surrounding granuloma. Fiber "blocking" of the

Downloaded At: 09:58 22 January 2011

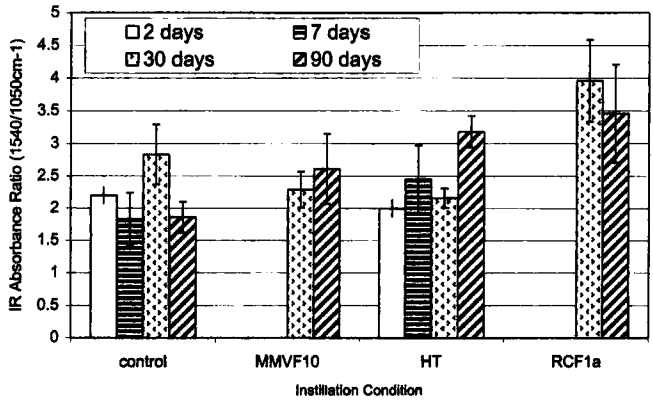

FIGURE 7 Chart of IR absorbance ratios of the Amide II protein absorbance (1540 cm^{-1}) and the carbohydrate absorbance (1050 cm^{-1}) of rat lung tissue after instillation of phosphate-buffered saline (control) and vitreous fibers. Data are presented as averages ± standard deviations.

background chlorine signal from the tissue in which it embedded attests to the retained electron density of the structure, despite 30 days of apparently aggressive attack by particle-digesting cells.

Adjacent areas of these same tissues, which appeared fiber-free at the scanning electron microscopic level, often indicated below-surface vitreous fiber presence by the energy-dispersive X-ray signals seen for the major fiber elements.

Infrared spectra showed similar increases and persistence for other macrophage-related absorptions in RCF1a-instilled lungs, while the control specimens displayed – by both infrared and microscopic methods – diminishing macrophage involvement by the 90-day observation time.

In these latter cases, although more analysis is required to confirm this finding, the IR spectra also indicated the persistence of silica-related absorptions in the originally fiber-instilled lungs. Export of the products of dissolution of glass from lung tissues was not as rapid a process as fiber disappearance in the rats.

Downloaded At: 09:58 22 January 2011

TABLE II Results of differential blood analyses, showing average percentages of 5 types of leukocytes in blood of groups of test animals. Except where noted, $n = 3$ animals per group. [N: neutrophils, PMNs; L: lymphocytes; M: monocytes; EOS: eosinophils; BO: basophils]

Fiber type and	*Cells as percentage of Leukocytes present in blood*				
post-instillation time	*N*	*L*	*M*	*EOS*	*BO*
(PBS control)					
*2 days	17 ± 2	79 ± 1	2 ± < 1	2 ± 2	< 1
7 days	16 ± 4	80 ± 6	4 ± 2	< 1	< 1
92 days	22 ± 2	76 ± 1	< 1	2 ± 1	< 1
*$n = 2$					
MMFV 10					
91 days	12 ± 1	86 ± 1	1 ± 1	< 1	< 1
HT					
2 days	16 ± 3	83 ± 3	1 ± < 1	< 1	< 1
7 days	17 ± 4	80 ± 6	1 ± 1	2 ± 1	< 1
30 days	15 ± 4	83 ± 4	1 ± < 1	1 ± < 1	< 1
90 days	10 ± 3	84 ± 3	5 ± 2	1 ± < 1	< 1
RCF1a					
30 days	16 ± 2	80 ± 2	2 ± < 1	1 ± < 1	< 1
92 days	19 ± 5	77 ± 6	3 ± 2	1 ± < 1	< 1

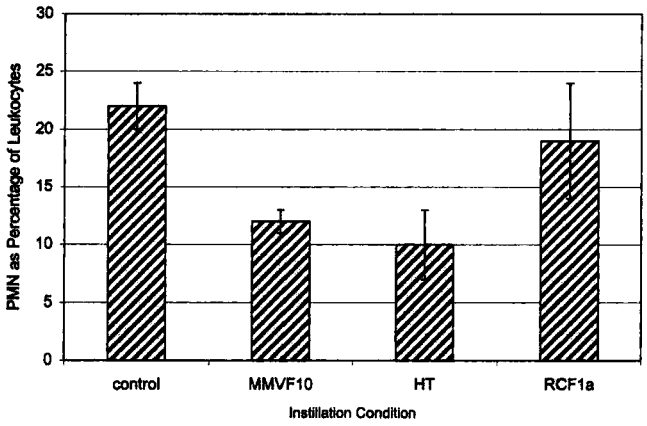

FIGURE 8 Percentage of PMN cells (polymorphonucleocytes, neutrophils) in leukocyte populations of blood samples from rats 90 days after instillation of phosphate-buffered saline (control) and vitreous fibers. Data are presented as averages ± standard deviations.

Downloaded At: 09:58 22 January 2011

Results of Differential Blood Analyses

Results of the differential blood analyses are summarized in Table II. From Table II, it is noted that percentages of the different types of leukocytes were relatively consistent within any particular group of animals, among post-instillation time periods, and between fiber types. Lymphocyte levels were particularly consistent across all groups. Figure 8, however, highlights a trend noted in percentages of polymorphonucleocytes (PMNs, or neutrophils) 90 days after instillation. It is seen that animals instilled with MMVF 10 or with HT fibers had fewer neutrophils in their blood than animals instilled with RCF1a or only the phosphate-buffered saline.

DISCUSSION

Instilled fibers of all three types usually were located within granulomatous cell clusters formed within 2 days of fiber instillation. HT fibers, uniquely, were broken down most rapidly into smaller segments at the sites of phagocytic cells attached along their lengths. These fibers otherwise were too long to be engulfed and internally

digested within the acidic granules of macrophages [1]. The observation that HT fibers not yet broken into smaller lengths showed local narrowing and loss of Prussian Blue-stainable substance mainly in regions with tightly attached phagocytes, is consistent with the finding by Carter [22] of external digestion of large particles by phagocytes converting to osteoclasts. Residual HT fragments were found to be depleted of constituents in proportion to the fibers' original elemental ratios, when examined by EDX-ray analysis. Early results from examination of the thoracic lymph nodes retrieved from HT-instilled rats confirm that fiber fragments were transported from the lung to the lymph nodes and possibly more peripheral locations.

Infrared imaging results obtained by colleagues at the National Institutes of Health, for representative lung specimens from this study, also identified the general lung tissue background to be collagen and glycoprotein-dominated "ground" substance, with some lipoidal surfactant. Granulomatous accretions had enhanced infrared absorptions in regions associated with carboxyl and nitroso groups, attributed to macrophages, as well as a small silicate band attributed to embedded glass fibers. Isolated glass fiber lengths protruding into lung vacuoles were surrounded by spread cells and had characteristic infrared spectra dominated by the silica absorption band and by macrophage-related bands; little collagen, glycoprotein, or fatty substance was present.

Infrared spectra of sequentially-harvested lung lobe slices, from rats living 2, 7, 30 and 90 days after glass fiber instillation, showed increasing ratios of absorption bands associated with granuloma formation only for RCF1a fibers at the final date. All specimens of fiber-instilled lungs continued to display silica absorption bands for the entire 90-day experimental periods, however. These findings show that the components of the rapid dissolution of the MMVF 10 insulation fiber and of the slower dissolved (shortened, then engulfed) HT stonewool remained predominantly within the lung tissue and were not exported to other organs in significant quantities. It is possible that dissolution-product-induced sequestration of PMNs within the lung, diminishing the numbers in circulation, accounts for the data displayed in Figure 8. Additional analyses of lymph nodes, liver, spleen, and kidney from the test animals are continuing, to investigate transport kinetics of instilled fibers or dissolution products from the lungs to these other organs.

Downloaded At: 09:58 22 January 2011

Results of this study with respirable vitreous fibers of known, controlled compositions suggest that all particles entering the lungs, in spite of initial encounters with similar extracellular fluid, matrix, surfactant and cellular types, can induce composition-dependent differential responses from the active phagocytic cells that surround them. The types of observations made in various tissue sites have recently been reviewed [23] and examined from the perspective of hypersensitivity induction [24]. A growing body of literature focuses on particles cast as wear debris into internal body tissues [25–27], illustrating the need for more distinct discrimination of the cellular/particle interactions in many body sites.

Most intriguing is the observation by Carter and co-workers [19, 22] that giant cells with osteoclast-like (mineral-dissolving) properties are preferentially induced by calcium–phosphate and other "digestible" particulate debris while giant cells induced by polymethylmethacrylate particles, polypropylene particles, or even by mineral talc particles, display features characteristic only of classical "foreign body" inflammatory polykarya, which do *not* degrade extracellular substrata. It is relevant that the quicker "clearing" HT fibers investigated here were calcium-rich, and also contained some phosphate. This evidence, linking material compositional properties to the induction of specific biological "clearing" responses, should be taken into account when evaluating new prosthetic devices that may generate wear debris during their functional correction of deformities, or pathological states, in human recipients. More such evidence must be gathered regarding the "inadvertent implants" of occupationally- or environmentally-generated particles that collect in the lung, and in other body sites.

The infrared spectroscopy results reported here, revealing generalized retention of dissolved particulate silica throughout the lung bed, require confirmation and extension with newer histopathologic staining techniques to identify morphological changes that could forecast later functional changes. Blood specimens taken from experimental animals at the times of lung harvest, when inspected for changes in white cell "differential" counts, were within the normal values reported for rats [17]. Since the blood of the rats in this study remained within the published broad range of "normal" blood chemistry, it is unlikely that the results reported here were confounded by any infectious, toxic, or other pathologic process.

Downloaded At: 09:58 22 January 2011

Yet, in comparison with the saline-instilled (control) rats in this study, an interesting pattern was seen that requires more studies to be verified. Whereas the saline-control and insoluble RCF1a fiber-instilled animals showed increases in circulating neutrophil abundance over the 90-day period, the more-soluble-fiber-instilled animals (MMVF10 and HT) showed decreases in neutrophil abundance, relative to control animals. This might be interpreted as preliminary evidence of an ongoing nontoxic but still "reactive" response of the lung tissue to dissolution products of fiberglass, while the saline control and insoluble particle-instilled lungs recovered more quickly from the initial ionic imbalance. Of equal interest and importance is the observation that the rat blood lymphocyte counts were essentially invariant over the whole experimental animal population, confirming and extending the findings that these animals remained immunologically uncompromised, throughout the study [17].

Downloaded At: 09:58 22 January 2011

The influences of the body's surface-active substances should not be neglected in considering how small particles are dealt with physiologically. Here, the lung provides a possibly extreme example. The surface properties of the lung's inner envelope are generally attributed to an abundant lipid (dipalmitoyl phosphatidylcholine, DPPC)-dominated material called "pulmonary surfactant" [28]. Pulmonary surfactant preparations made by chloroform–methanol extraction of cell-free brochoalveolar lavages of lungs of freshly-killed calves improve lung mechanics significantly in both premature lambs and human infants [29], and display surface tensions as low as 42 mN/m. Our research group has performed preliminary Langmuir-Adam trough experiments on lung surfactant interactions with vitreous fibers. Lung surfactants concentrated at the air/water interface (*in vitro*) reduced the surface tension of pure water and salt-solutions to the same low values, and triggered the aqueous-phase engulfment (sinking) of the respirable glass fibers used here that otherwise were retained at the air/water interface. Similar results were obtained with asbestos fibers.

New techniques are required to make measurements within harvested lung tissues, macrophages from lung lavages, and additional harvested animal specimens to test hypotheses on the environment and fate of instilled vitreous fibers and other particle types unambiguously. Animal trials must be extended to examine consequences of respirable

fiber inhalation *versus* intratracheal instillation. Extrapolation to events associated with similar particles impacting ocular tissues [30] must be done with care.

It is important that the required methods be advanced quickly. Alveolar macrophages undergo various morphological and surface changes upon contact with different particulate substrata, including glass, aluminum foil and cotton [31, 32], and similar changes have been noted from humans having occupational exposures to inorganic particles, including asbestos, silica, and coal [33].

Production of particulate wear debris is an inevitable consequence of the implantation of alloplastic materials into loaded human joints, sometimes with tragic sequelae as in the universal failure of certain TMJ (temporomandibular joint; jaw joint) implants fabricated from silicone, fluorocarbon, hydrocarbon, metallic, and mineral constituents [19, 34]. It is a regulatory necessity that the required database on particle-tissue interactions be significantly expanded. Similarly, since acute and chronic respiratory distress syndromes can develop from inadvertent contact, adhesion, and uptake of aerosolized diesel exhaust particulates and even dental drill particulates entering the lung [35], there is a strong demand for these data in environmental health fields, as well [36].

Downloaded At: 09:58 22 January 2011

CONCLUSION

Particle contact-induced differentiation of a host's reacting cell populations can follow alternate paths with separate end points responsive to the specific surface chemistries of the contacting materials themselves. In all cases of particle intrusion to the body, it is critical to detect and decipher the relationships between the surface properties of the particles and the receiving biofluid/cells at the instant of effective contact. Independent documentation of the identity of those particles engulfed and modified by the cellular bodies also is important, to prevent attribution of negative consequences to an improperly identified material. It is possible, for example, that differentiation of blood monocytes into either macrophages, which engulf and digest particles internally, or osteoclast-like phagocytes, which can acid-digest nonengulfable particles externally, depends on the calcium–phosphorus contents of implanted mineral debris.

Acknowledgments

This work was supported by the Industry/University Cooperative Research Center for Biosurfaces (IUCB), and used respirable fiberglass particles donated by industry members of IUCB. We thank Dr. Pina Colarusso (National Heart, Lung, and Blood Institute; Laboratory of Kidney and Electrolyte Metabolism) for IR microscopic and synchrotron analyses of lung sections. We also are grateful to Dr. Bruce Holm and Dr. Edmund Egan of the University at Buffalo, who provided expert advice on lung surfactant and lung cell harvest.

References

[1] Eastes, W. and Hadley, J. G., *Inhal. Toxicol.* **8**, 323 (1996).
[2] Hesterberg, T., Miller, W., Hart, G., Bauer, J. and Hamilton, R., *J. Occup. Health Safety* **12**, 345 (1996).
[3] Yu, C. P., Dai, Y. T., Boymel, P. M., Zoitos, B. K., Oberdorster, G. and Utell, M. J., *Inhal. Toxicol.* **10**, 253 (1998).
[4] Hesterberg, T. W., Axten, C., McConnell, E. E., Oberdorster, G., Everitt, J., Miller, W. C., Chevalier, J., Chase, G. R. and Thevenaz, P., *Environ. Health Perspectives* **105**(Supp. 5), 1223 (1997).
[5] Hesterberg, T. W., Hart, G. A., Chevalier, J., Miller, W. C., Hamilton, R. D., Bauer, J. and Thevenaz, P., *Toxicol. Appl. Pharmacol.* **153**, 68 (1998).
[6] Kamstrup, O., Davis, J. M. G., Ellehauge, A. and Guldberg, M., *Ann. Occup. Hyg.* **42**, 191 (1998).
[7] Hesterberg, T. W., Chase, G., Axten, C., Miller, W. C., Musselman, R. P., Kamstrup, O., Hadley, J., Morscheidt, C., Bernstein, D. M. and Thevenaz, P., *Toxicol. Applied Pharmacol.* **151**, 262 (1998).
[8] Potter, R. M. and Mattson, S. M., *Glastech. Ber.* **64**, 16 (1991).
[9] Mattson, S. M., *Ann. Occup. Hyg.* **38**, 857 (1994).
[10] Eastes, W. and Hadley, J. G., *Inhal. Toxicol.* **7**, 179 (1995).
[11] Bernstein, D. M., Morscheidt, C., Grimm, H.-G., Thevenaz, P. and Teichert, U., *Inhal. Toxicol.* **8**, 345 (1996).
[12] Eastes, W., Morris, K. J., Morgan, A., Launder, K. A., Collier, C. G., Davis, J. A., Mattson, S. M. and Hadley, J. G., *Inhal. Toxicol.* **7**, 197 (1995).
[13] Mattson, S. M., *Environ. Health Perspectives* **102**(Supp. 5), 87 (1994).
[14] Eisner, D. A., Kenning, N. A., O'Neill, S. C., Pocock, G., Richards, C. D. and Valdeolmillos, M., *Pflugers Arch.* **413**, 553 (1989).
[15] Seksek, O., Henry-Toulme, N., Sureau, F. and Bolard, J., *Analytical Biochem.* **193**, 49 (1991).
[16] Baier, R. E. and Meyer, A. E., *Intl. J. Oral Maxillofac. Implants* **3**, 9 (1988).
[17] Harkness, J. E. and Wagner, J. E., *The Biology and Medicine of Rabbits and Rodents* (Lea & Febiger, Publishers, Philadelphia, 1989), p. 49.
[18] Paschalis, E. P., Boskey, A. L. and Nancollas, G. H., *Advances in Materials Sciences and Implant Orthopedic Surgery* (Kluwer Academic Publishers, Amsterdam, 1995), pp. 47–60.
[19] Carter, L. C., Carter, J. M., Nickerson, P. A., Baier, R. E., Wright, J. R. and Meenaghan, M. A., *J. Adhesion* **74**(1–4), 53–77 (2000).
[20] Coleman, D. L., King, R. N. and Andrade, J. D., *J. Biomed. Mater. Res.* **8**, 199 (1974).

Downloaded At: 09:58 22 January 2011

[21] Baier, R. E., Meyer, A. E., Natiella, J. R., Natiella, R. R. and Carter, J. M., *J. Biomed. Mater. Res.* **18**, 337 (1984).
[22] Carter, L. C., Analysis of the Cellular Healing Response of the Chick Chorioallantoic Membrane to Implanted poly(Glycolic Acid). Doctoral Dissertation. State University of New York at Buffalo (1993).
[23] Carter, L. C., *Handbook of Biomaterials Evaluation* (Taylor & Francis, Philadelphia, 1999), Chap. 14, pp. 241–252.
[24] Merritt, K., *Handbook of Biomaterials Evaluation* (Taylor & Francis, Philadelphia, 1999), Chap. 18, pp. 291–300.
[25] Goodman, S. B., Lind, M., Song, Y. and Smith, R. L., *Clin. Orthopaed. Related Res.* **352**, 25 (1998).
[26] Santerre, J. P., Labow, R. S. and Boynton, E. L., *Canadian J. Surgery* **43**, 173 (2000).
[27] Brown, S. L., Silverman, B. G. and Berg, W. A., *Lancet* **350**, 1531 (1997).
[28] Holm, B. A. and Matalon, S., *Anesth. Analg.* **69**, 805 (1989).
[29] Notter, R. H., Egan, E. A. and Kwong, M. S., *Pediatr. Res.* **19**, 569 (1985).
[30] Stokholm, J., Norn, M. and Schneider, T., *Scand. J. Work Environ. Health* **8**, 185 (1982).
[31] Leake, E. S. and Wright, M. J., *J. Reticuloendothelial Society* **25**, 417 (1979).
[32] Leake, E. S., Wright, M. J. and Myrvik, Q. N., *J. Reticuloendothelial Society* **17**, 370 (1975).
[33] Takemura, T., Rom, W. N., Ferrans, V. J. and Crystal, R. G., *Am. Rev. Respir. Dis.* **140**, 1674 (1989).
[34] Baier, R., Axelson, E., Meyer, A., Carter, L., Kaplan, D., Picciolo, G. and Jahan, M., *J. Adhesion* **74**(1–4), 79–101 (2000).
[35] Mazzarella, M. A. and Flynn, D. D., *An Introduction to Experimental Aerobiology* (Wiley-Interscience, New York, 1969), Chap.18, pp. 437–462.
[36] Effros, R. M., *Inhalation Aerosols: Physical and Biological Basis for Therapy* (Marcel Dekker, Inc., New York, 1996), Chap. 5, pp. 139–154.

Downloaded At: 09:58 22 January 2011